Catalysis Today 148 (2009) 290–297

Contents lists available at ScienceDirect

Catalysis Today

journal homepage: www.elsevier.com/locate/cattod

A comparison of mixed-conducting oxygen-permeable membranes for CO_2 reforming

David A. Slade, Qiying Jiang, Karen J. Nordheden, Susan M. Stagg-Williams *

Chemical and Petroleum Engineering, University of Kansas, 1530 W. 15th Street, Lawrence, KS 66045, USA

ARTICLE INFO

Article history:
Available online 27 September 2009

Keywords:
CO_2 reforming
SFC
BSCF
Mixed-conducting ceramic membranes

ABSTRACT

$SrFeCo_{0.5}O_x$ (SFC) and $Ba_{0.5}Sr_{0.5}Co_{0.8}Fe_{0.2}O_x$ (BSCF) ceramic membranes have been evaluated for the CO_2 reforming of CH_4 at 800 °C over a Pt/ZrO_2 and a $Pt/CeZrO_2$ (17.5 wt% Ce) catalyst. The SCF membrane was a dense membrane approximately 2 mm thick while the BSCF membrane had a 400 μm dense layer supported on a 2.2 mm porous BSCF layer. Both membranes exhibited good mechanical integrity and stability under reaction conditions, and the membrane effect on methane conversion was roughly proportional to the apparent oxygen production of the membranes. Methane conversion and water production increase simultaneously in the presence of the membrane and the membranes improve catalyst longevity as well as activity. Results suggest that membrane oxygen reacts with hydrogen at the membrane surface to form water that can then participate in the reaction set via steam reforming. Among the combinations of membrane and catalyst tested, the $Pt/CeZrO_2$ catalyst on the BSCF membrane produced the highest methane conversion and H_2:CO ratios as well as the most water. This test also yielded the greatest net membrane oxygen production, with more than three times the oxygen production of the BSCF test with the Pt/ZrO_2 catalyst. The SFC membranes exhibited steady state net oxygen production of zero or less. Negative membrane oxygen production values are attributed to the reduction of CO_2 to CO on the membrane surface with incorporation of the oxygen into the membrane material.

1. Introduction

Hydroformylation and Fischer–Tropsch reactions require synthesis gas (syngas) feedstocks with specific hydrogen to carbon monoxide ratios in the range of 1–2. As syngas is conventionally produced by steam reforming or partial oxidation reactions that produce H_2:CO ratios of two or greater, CO_2 reforming with its stoichiometric H_2:CO ratio of one is a potentially useful sidestream reaction for decreasing the ultimate ratio to meet the downstream target values less than two. CO_2 reforming has not received widespread commercial attention, in part because of catalyst deactivation issues related to the use of CO_2 as the oxygen source of the reaction and the resulting tendency for carbon deposition [1,2].

Oxygen-assisted CO_2 reforming and autothermal reforming have been explored with the goals of reducing the energy demands of steam and CO_2 reforming, "tuning" the H_2:CO ratio by manipulating the ratio of O_2 and CO_2 in the reactor feed, and increasing catalyst life by reducing carbon deposition [1,2]. However, this option requires pure oxygen as a feedstock, and an energy-intensive air separation unit can represent substantial capital and operating costs. For example, about one-third of a methane partial oxidation (POM) synthesis gas facility's operating costs and up to 40% of its capital costs can come from the air separation unit alone [3].

Because of the high costs associated with pure oxygen, oxygen-permeable ceramic membranes have been explored as an alternative oxygen source for hydrocarbon conversion reactors [3–7]. These non-porous ceramic materials allow the conduction of oxygen ions through the lattice of the solid material resulting in 100% selectivity for oxygen. The mixed-conducting materials of interest for membrane reactor applications conduct electrons as well as oxygen ions, so they require only high temperature and an imposed oxygen potential gradient to exhibit oxygen flux. If an oxygen-conducting ceramic membrane were used in place of co-fed gas-phase oxygen, the benefits of oxygen-assisted CO_2 reforming could be attained while eliminating the costs associated with gas-phase oxygen.

Membrane-supplied oxygen incorporates several significant environmental benefits over gas-phase oxygen supplies for synthesis gas operations: (1) a substantial reduction in energy consumption; (2) safer oxygen (no hotspot or flammability issues); (3) inherently distributed oxygen introduction which can reduce overall oxygen consumption, increase the selectivity of oxidation reactions [8], and produce a more uniform and predictable reactor

* Corresponding author at: Chemical and Petroleum Engineering, University of Kansas, 1530 W. 15th Street, Room 4132 Learned Hall, Lawrence, KS 66045, USA. Tel.: +1 785 864 2919; fax: +1 7875 864 4967.
E-mail address: smwilliams@ku.edu (S.M. Stagg-Williams).

0920-5861/$ – see front matter © 2009 Elsevier B.V. All rights reserved.
doi:10.1016/j.cattod.2009.08.016

temperature profile; and (4) minimized occurrence of homogeneous thermochemical reactions involving O_2 which can produce soot-forming precursors [9].

Mixed-conducting ceramics have typically been investigated for use with partial oxidation of methane (POM) because of its appropriately high operating temperatures and the strongly reducing environment created by the POM reactions. However, the reducing reaction environment and high operating temperature of CO_2 reforming might also allow effective use of a membrane reactor. Studies of less stable oxygen-permeable ceramics have shown that adding CO_2 to the permeate-side feed stream can reduce instances of membrane fracturing [10], indicating that CO_2 reforming might be a more appropriate reaction choice in general for ceramic membrane reactors. Furthermore, the smaller oxygen requirement of oxygen-assisted CO_2 reforming increases the list of candidate ceramics to include a selection of mechanically stable membrane materials whose oxygen flux limitations preclude their use in the POM reaction [7].

Two mixed oxide membrane materials are compared in this work: the non-perovskite $SrFeCo_{0.5}O_x$ and the perovskite $Ba_{0.5}Sr_{0.5}Co_{0.8}Fe_{0.2}O_x$ referred to henceforth as SFC and BSCF, respectively. SFC falls into the low flux, high stability category and BSCF falls into the category of high flux membrane candidates. The SFC membranes used for reaction testing were conventional dense membranes approximately 2 mm in thickness while the BSCF membranes were asymmetric bilayer membranes with a thin dense layer (~400 μm) on a porous BSCF support. The bilayer structure enhances oxygen flux through the membrane by decreasing the solid state diffusion path length through the dense layer.

Two platinum catalysts were used in the reaction studies: 0.43 wt% Pt/ZrO_2 and 0.42 wt% $Pt/CeZrO_2$ (18 wt% Ce). The Pt/ZrO_2 catalyst was chosen because it has been studied previously for CO_2 reforming in conventional quartz tube PFR reactors [1,7,11] and has been shown to have low activity and to deactivate quickly. These attributes allow any improvement to be seen more readily because the catalyst is certain to operate well below equilibrium for all tests and to deactivate quickly.

After the effectiveness of the membranes was established with the Pt/ZrO_2 catalyst, the $Pt/CeZrO_2$ catalyst was tested. The $CeZrO_2$ support was chosen because they have been shown to exhibit higher activity than ZrO_2 as well as reduced deactivation rates [1,12]. These benefits have been attributed to the ability of ceria-promoted zirconia to be repeatedly reduced and oxidized and thereby to act as an "oxygen sink" and thereby facilitate carbon removal from catalytic metal particles. This labile oxygen trait is a less dramatic version of the distinguishing characteristic of the ceramic membrane materials featured in this work and should therefore influence the effect of any oxygen in the reaction chamber, whether provided by a membrane or in the gas phase.

2. Experimental methodology

2.1. Membrane reactor overview

All reaction and flux tests were performed in a two-sided concentric quartz tube membrane reactor shown in Fig. 1. The reactor seals against both sides of the test membrane with gold ring gaskets between the outer quartz tubes and the membrane surfaces and an external pneumatic press to maintain constant compressive force at all times. The gold gaskets soften as the reactor system approaches the 800 °C reaction temperature and the seal is fully formed within 30 min at 800 °C. Prior to reaction, the amount of leaked air is assessed by mass spectrometer monitoring of nitrogen in the reactor effluent. Increasing the temperature to 850 °C does not improve the seal.

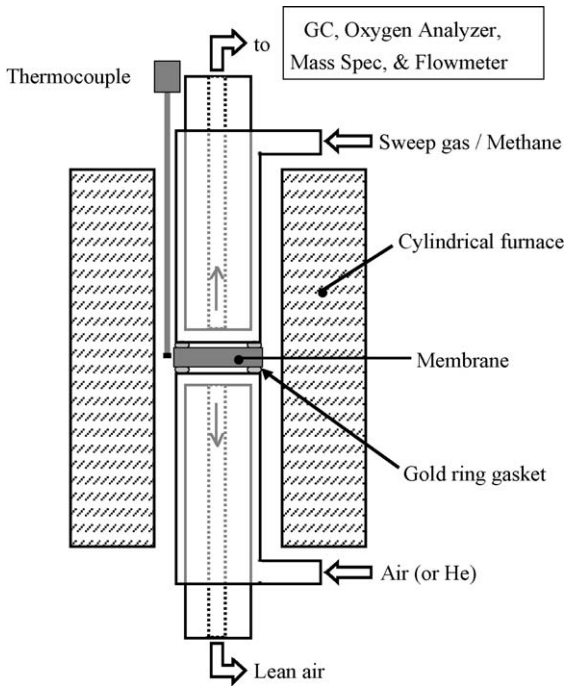

Fig. 1. Membrane reactor system.

In all cases, the leak around the gold gaskets during operation was estimated as less than 0.3% of the reactor feed flowrate. However, it is important to note that substantial leakage during reactor heat-up is unavoidable before the gold seals soften sufficiently. Air incursion during the temperature ramp can comprise as much as 5% of the argon sweep gas (or 1% O_2) until the seal forms at 800 °C. It is assumed that the catalyst bed is exposed to this amount of oxygen during preliminary heating.

In addition to the ceramic membranes, a stainless steel "blank" membrane painted with an inert BN_3 paint to prevent reaction on the steel surface is used as an inert control to provide baseline data for the ceramic membrane experiments.

2.2. SFC dense membrane preparation

The SFC powder was obtained from Praxair Specialty Ceramics. The dense, disk-shaped SFC ceramic membranes were pressed at 60 MPa for 3 min in a uniaxial press and then sintered at 1180 °C in flowing air for 10 h. Prior to pressing, the SFC powder was passed through a 60-mesh sieve and then coated with a liquid binder solution of 1 wt% ethylcellulose in a solvent mixture of acetone and ethanol. The coated powder was heated gently with continuous stirring until the solvents were entirely evaporated.

2.3. BSCF asymmetric membrane preparation

BSCF powders were prepared in house by the citrate-EDTA (ethylenediaminetetraacetic acid) method [13]. Stoichiometric quantities of the nitrate salts of barium, strontium, cobalt, and iron were added to EDTA-$NH_3{\cdot}H_2O$ solution followed by citric acid. The molar ratio of total metal ion (Ba, Sr, Co, Fe) to EDTA to citric acid was 1:1:1.5. The pH of the solution was adjusted to 6 by adding $NH_3{\cdot}H_2O$. With heating and stirring, a dark purple gel was formed. The gel was heated and dried in the air at 110–120 °C to yield the preliminary powder. The preliminary powder was calcined at 950 °C for 5 h in a muffle furnace to obtain BSCF powder.

The bilayer BSCF membrane disks were prepared using the same uniaxial press and cylindrical die as used for the SFC

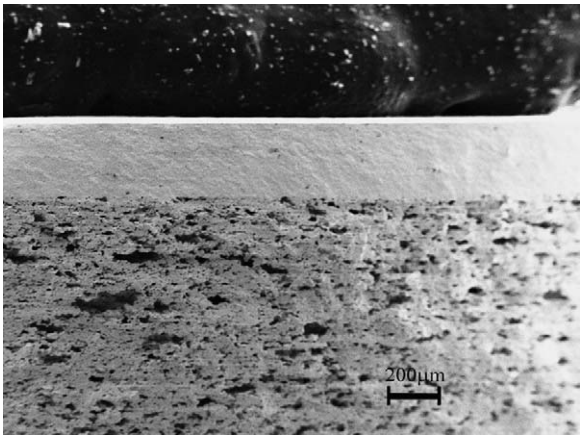

Fig. 2. SEM micrograph of a bilayer BSCF membrane (cross-section).

membranes. To form the dense layer, BSCF powder was added to the die and the powder surface was gently leveled off and compressed using the press. For the porous layer, a uniform mixture of carbon fibers (TohoTenax, 7 μm diameter), ethylcellulose powder, and additional BSCF powder was prepared. This mixture was added to the die on top of the lightly compressed plain BSCF powder. The bilayer powders were then pressed at 250 MPa for 5 min to form the green BSCF asymmetric membranes. Finally, the membranes were sintered at 1100 °C for 5 h with a ramping and cooling rate of 1 °C/min. The carbon fibers and ethylcellulose powder burn out during the heating ramp, thereby forming the porous support layer for the thin dense layer.

The morphology of a typical bilayer BSCF membrane is shown in Fig. 2. A clean interface between the dense layer and the porous substrate can be observed, as can both the density of the top layer and the porosity of the support layer. The dense layers in the sintered membranes were about 400 μm thick and the porous support layers were about 2.2 mm thick. Decreasing the thickness of the dense layer through the use of the porous support layer has been shown to produce greater oxygen permeation through the membrane with the increase in oxygen permeation ascribed to the decrease in dense layer thickness and the resulting increase in oxygen gradient across the dense layer [14].

2.4. Catalyst preparation

Both catalysts were prepared by the incipient wetness impregnation method. Catalyst from a single batch was used in all tests of a particular catalyst. The ZrO_2 and the $CeZrO_2$ (18 wt% Ce) support materials were obtained from Magnesium Elektron, Inc. (MEI) and both catalysts were prepared by the same procedure. The supports were calcined at 800 °C prior to platinum deposition using an aqueous solution of $H_2PtCl_6{\cdot}6H_2O$. After deposition the loaded catalysts were dried overnight at 120 °C and then calcined at 400 °C for 2 h in flowing air. For the Pt/ZrO_2 and $Pt/CeZrO_2$ catalysts, BET single point surface area analysis indicated a support surface area of 29 and 48 m^2/g, respectively, and TEM was used to confirm that the platinum particles were highly dispersed (21% and 23%, respectively). Additional information about the preparation and characterization of the catalysts can be found elsewhere [1]. No catalyst reduction procedure was performed prior to CO_2 reforming reaction testing in the membrane reactor.

2.5. Reaction test parameters

All membrane reaction tests were conducted with identical operating conditions. 10 mg of supported platinum catalyst powder was spread evenly in a thin layer (~1 mm) across the entire portion of the membrane or stainless steel blank surface that is exposed within the reactor's outer quartz tube. This small quantity of catalyst minimizes transport limitations within the catalyst layer and ensures good proximity between the membrane material and the entire catalyst bed. It has the additional advantage of immediately exposing catalyst deactivation trends by allowing the reactors to operate well below equilibrium conversion levels. Fig. 3 provides a schematic depiction of the SFC membrane under operating conditions.

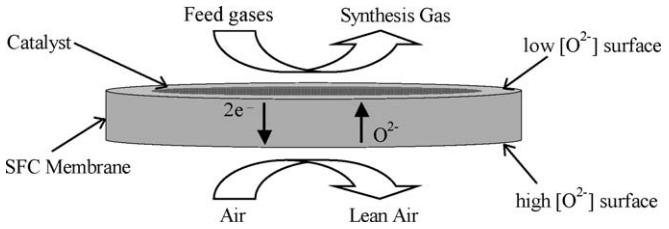

Fig. 3. Ceramic membrane under reaction conditions with powder catalyst.

A CH_4:CO_2 ratio of 1:1 was used in all cases with 20 mol% argon comprising the remainder of the feed stream. The feed flowrate was 25 mL/min, which corresponds to a modified space velocity of 150 L/h/$g_{catalyst}$. Continually replenished atmospheric pressure air was used as the oxygen supply across the bottom membrane surface.

After reaching 800 °C, the reactor was held at this temperature with 100% argon feed to allow the softened gold gaskets to seat themselves and the membrane to equilibrate fully under the imposed air:argon oxygen gradient. To ensure comparable pre-reaction conditions for the powder catalysts, a 2-h hold at 800 °C was also imposed for stainless steel blank membrane tests. After sealing the reactor at 800 °C but prior to flux testing, all membranes were tested for cracks or porosity by flowing lightly pressurized helium through the air supply side of the membrane reactor. The mass spectrometer output was examined for changes in the helium signal. No helium penetration was detected at 800 °C in any of the tests either immediately before or immediately after the reaction test period.

2.6. Analytical procedures

Reactor effluent composition was quantified at 30-min intervals during CO_2 reforming tests using an SRI 8100 Gas Chromatograph with FID for carbon-containing compounds and TCD for H_2 and N_2. Effluent was also monitored qualitatively and continuously using a Balzers OmniStar quadrapole mass spectrometer both to confirm and interpolate trends observed in the GC data and to provide important additional information including pre-reaction oxygen flux data. In addition, effluent flowrate and oxygen level were monitored continuously using an Agilent ADM2000 volumetric flowmeter and an AMI Model 60 oxygen sensor.

Effluent water was calculated from a hydrogen atom balance and the resulting trends were confirmed by mass spectrometer data. After closing the hydrogen balance, membrane oxygen flux was estimated from an oxygen atom balance.

3. Results and discussion

3.1. Baseline membrane oxygen fluxes

Oxygen flux data were acquired for both membrane types under an air:argon gradient and the results are shown in Fig. 4. Steady state oxygen production was estimated from mass spectrometer data at 50 °C intervals. Fig. 4 shows that the oxygen flux for the bilayer BSCF asymmetric membrane at 800 °C is more

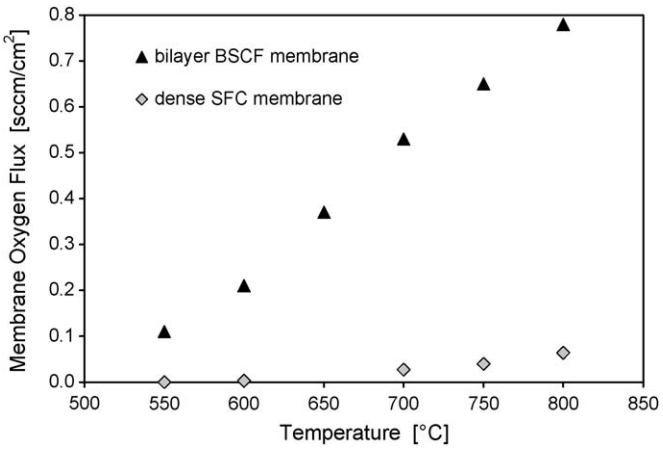

Fig. 4. Membrane oxygen permeation flux with an air:argon gradient.

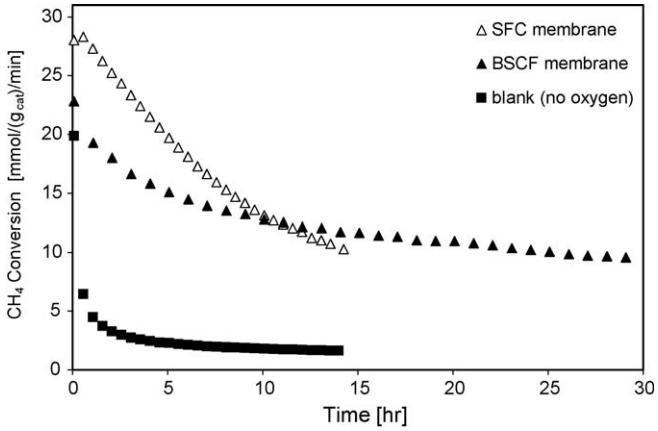

Fig. 5. Methane conversion with the Pt/ZrO_2 catalyst during CO_2 reforming at 800 °C. Feed flow is: 10 mL/min CH_4, 10 mL/min CO_2, and 5 mL/min argon; space velocity of 150 L/h/$g_{catalyst}$.

than ten times the flux through the SFC membrane. As a reference for the reaction testing that follows, the 800 °C flux for the bilayer BSCF membrane under an air:argon oxygen gradient represents 5.2% of a 25 mL/min reactor feed while the 800 °C SFC flux represents 0.43% of the same reactor feed.

3.2. CO_2 reforming with membranes only

The inherent catalytic activity of both the dense SFC membrane and the asymmetric BSCF membrane for the CO_2 reforming reaction was assessed by conducting the standard reaction test without including the powder catalyst. For these tests, CH_4 conversion was very low and minimal CO and H_2 were detected (<0.1 mol%), indicating that neither membrane material has significant inherent catalytic activity for methane conversion. Because CO_2 in the effluent actually increased in an almost 1:1 ratio with the limited amount of CH_4 conversion, the methane conversion that did occur can be ascribed almost entirely to combustion.

In addition to the two ceramic membrane types, a stainless steel blank test with no catalyst produced similarly low methane conversion. Fractional methane conversions ranged between 0.1% and 0.4% for the blank and between 0.1% and 0.6% for the membranes. These results confirm that neither membrane material is significantly more active for reforming reactions than the inert-coated stainless steel blank.

3.3. Test results with the Pt/ZrO_2 catalyst

The Pt/ZrO_2 catalyst shows higher CH_4 conversion with both ceramic membranes than with the stainless steel blank (Fig. 5). On average, it also shows lower relative CO_2 conversion (i.e., the ratio of moles of CO_2 converted to moles of CH_4 converted), higher H_2:CO ratios, and lower relative water production on the membranes than on the blank (Figs. 6–8, respectively). However, at the end of the 14 h test period, all three ratios for the SFC test approach their counterparts for the blank test.

This convergence late in the test period could be interpreted as evidence that the effect of the SFC membrane is diminishing to zero as the test progresses. However, methane conversion remains significantly greater throughout the test period on the SFC membrane than on the blank. The reaction profile trends for the blank test also remain constant throughout most of the test period while the reaction trends on the blank change throughout. The reaction profile on the SFC membrane thus differs from that on the stainless steel blank.

With the BSCF membrane, relative water production is initially higher than with the SFC membrane, while methane conversion is lower. Water production with the SFC membrane ultimately exceeds that of the BSCF membrane test, but the H_2:CO ratio with the Pt/ZrO_2 catalyst on the BSCF membrane remains significantly higher than on the SFC membrane. Also, CO_2 conversion is dramatically lower and much steadier on the BSCF membrane.

One possible conclusion from these trends is that a significant amount of combustion occurs on the BSCF membrane. This would explain the lower CO_2 conversion and steadily increasing water production results. However, combustion does not explain an increase in relative water production with a combination of decreasing methane conversion and steady relative CO_2 conversion. Neither does Reverse Water-Gas Shift (RWGS), which would require an increase in relative CO_2 conversion to produce the observed increase in relative water production.

A more comprehensive explanation assumes continuous oxidation of hydrogen on the membrane surface. The resulting water then contributes to methane conversion via steam reforming, which explains the higher H_2:CO ratios than observed on the SFC membrane with its lower initial water production. To the extent that it occurs, methane conversion by steam reforming replaces methane conversion by CO_2 reforming, leading to lower relative CO_2 conversion. The proposed steam reforming contribution diminishes over time, but hydrogen oxidation on the membrane, which is a separate phenomenon, appears to remain

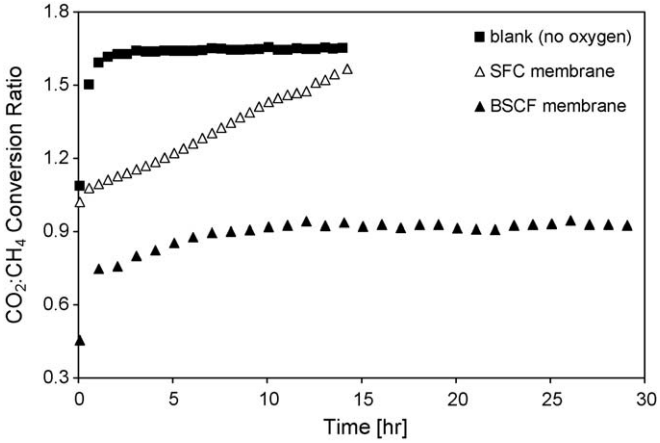

Fig. 6. Relative CO_2 conversion with the Pt/ZrO_2 catalyst during CO_2 reforming at 800 °C. Feed flow is: 10 mL/min CH_4, 10 mL/min CO_2, and 5 mL/min argon; space velocity of 150 L/h/$g_{catalyst}$.

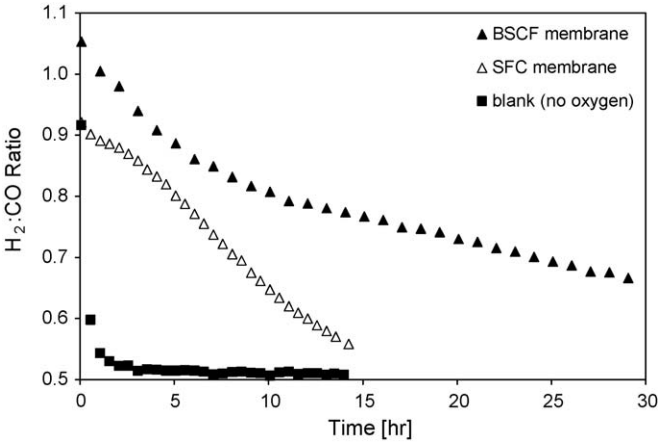

Fig. 7. H_2:CO ratios with the Pt/ZrO_2 catalyst during CO_2 reforming at 800 °C. Feed flow is: 10 mL/min CH_4, 10 mL/min CO_2, and 5 mL/min argon; space velocity of 150 L/h/$g_{catalyst}$.

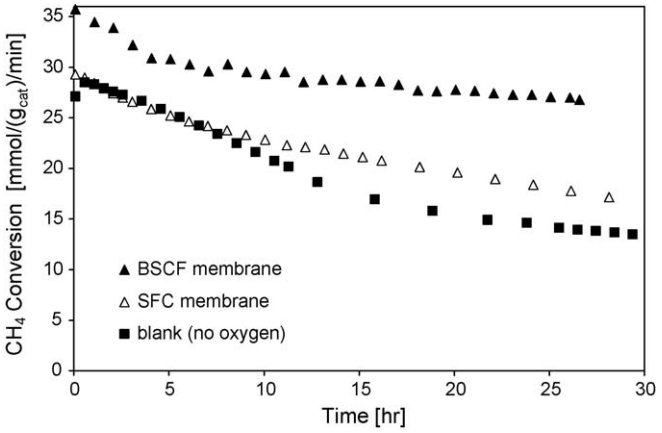

Fig. 9. Methane conversion with the $Pt/CeZrO_2$ catalyst during CO_2 reforming at 800 °C. Feed flow is: 10 mL/min CH_4, 10 mL/min CO_2, and 5 mL/min argon; space velocity of 150 L/h/$g_{catalyst}$.

constant. This causes the H_2:CO ratio to decrease along with methane conversion, as observed in Figs. 5 and 7. If water is produced at a constant rate while methane conversion decreases, relative water production should increase as indicated in Fig. 8.

Steam reforming with water produced from hydrogen at the BSCF membrane surface also would explain the lower relative CO_2 conversion with BSCF. If the water were produced via RWGS, relative CO_2 conversion would increase along with water production and the H_2:CO ratio should be lower than observed with the BSCF membrane. It does not appear that RWGS is a significant contributor to the initial reaction profile with the BSCF membrane but it could play an increasing role as the test progresses.

In contrast to the BSCF membrane, the SFC membrane results do imply such a Reverse Water-Gas Shift scenario: i.e., increasing relative CO_2 conversion with a commensurate increase in water production and sharply dropping H_2:CO ratios. Collectively, these trends indicate increasing RWGS activity relative to the amount of methane conversion on the SFC membrane as the test progresses and methane conversion decreases.

Previous studies and ongoing work have shown that oxygen species on the surface of the membranes readily react with hydrogen [7], which supports the conclusion that hydrogen oxidation on the membrane surface is the cause of increasing water production over time in the membrane tests. Hydrogen in the reaction chamber is more likely to remove individual oxygen atoms from the membrane than those atoms are to form molecular oxygen and evolve into the gas phase in the presence of hydrogen. This hypothesis applies to both membrane types.

3.4. Test results with the $Pt/CeZrO_2$ catalyst

As expected, the $Pt/CeZrO_2$ catalyst shows different methane conversion trends than the Pt/ZrO_2 catalyst both with and without the ceramic membranes, and the difference between the two membrane types is much greater with $Pt/CeZrO_2$ (Fig. 9). Interestingly, with this catalyst the low flux SFC membrane shows no improvement over the stainless steel blank until midway through the test period (Fig. 9). Even then, relative CO_2 conversion (Fig. 10) was nearly identical throughout for these two tests, as were H_2:CO ratio (Fig. 11) and relative water production results (Fig. 12). It appears that even after the effect of the SFC membrane began to manifest itself with the $Pt/CeZrO_2$ catalyst, the reaction profile did not change. This is an important difference from the effect of the SFC membrane on the Pt/ZrO_2 catalyst.

The fact that the $CeZrO_2$ support can be reduced and oxidized leads to one interpretation of the delayed and different effect of the SFC membrane on this catalyst. If, as proposed in the literature, the improved methane conversion activity of the $Pt/CeZrO_2$ catalyst is a result of the redox capability of the $CeZrO_2$ support, then this capability actually parallels the presumed oxygen transport

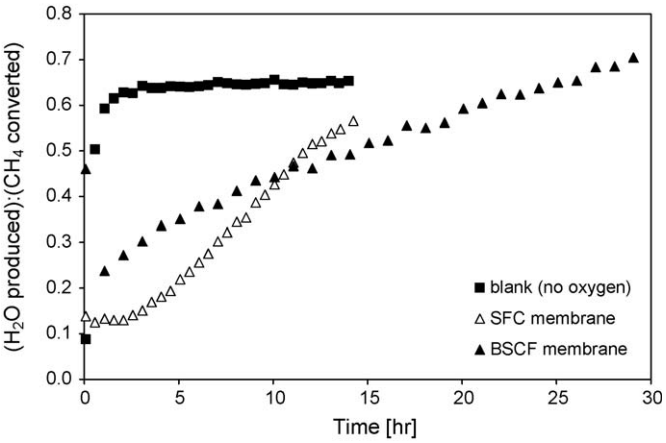

Fig. 8. Relative water production with the Pt/ZrO_2 catalyst during CO_2 reforming at 800 °C. Feed flow is: 10 mL/min CH_4, 10 mL/min CO_2, and 5 mL/min argon; space velocity of 150 L/h/$g_{catalyst}$.

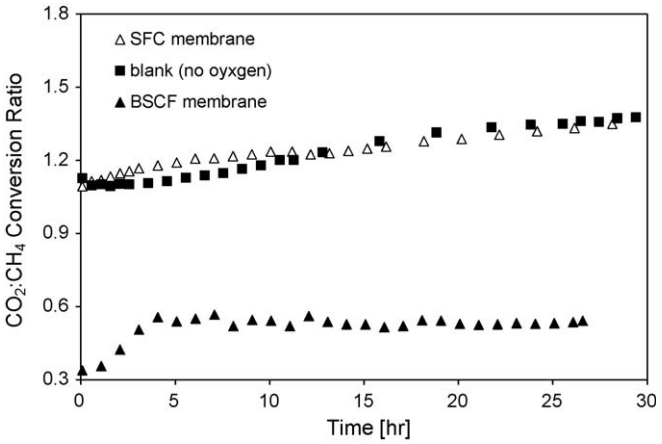

Fig. 10. Relative CO_2 conversion with the $Pt/CeZrO_2$ catalyst during CO_2 reforming at 800 °C. Feed flow is: 10 mL/min CH_4, 10 mL/min CO_2, and 5 mL/min argon; space velocity of 150 L/h/$g_{catalyst}$.

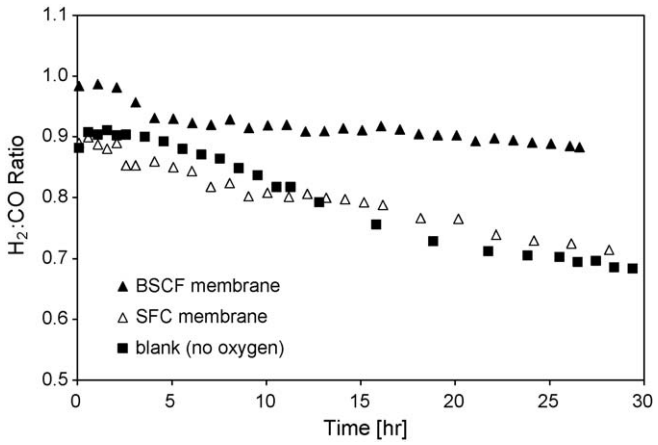

Fig. 11. H_2:CO ratios with the Pt/$CeZrO_2$ catalyst during CO_2 reforming at 800 °C. Feed flow is: 10 mL/min CH_4, 10 mL/min CO_2, and 5 mL/min argon; space velocity of 150 L/h/$g_{catalyst}$.

mechanism of the ceramic membranes. The catalyst could therefore be active enough initially to suppress the effect of the low flux SFC membrane. Over time, the $CeZrO_2$ support could be reduced by ambient hydrogen to the point that its ability to enhance methane conversion diminishes noticeably. At this point, the SFC membrane begins to have a detectable effect, causing methane conversion with the SFC membrane to diverge from that with the blank without changing the reaction profile. Because no net oxygen is supplied by the SFC membrane over this period (see Fig. 14), the mode of action of the SFC membrane would seem to be either similar to, or supportive of, the mode of action of the $CeZrO_2$ support in promoting catalytic activity.

This hypothesis explains why the relative CO_2 conversion, H_2:CO ratio, and relative water production trends (Figs. 10–12) are so similar for the membrane and the blank even as the methane conversion trends in Fig. 9 diverge. It also provides an explanation for the net zero membrane oxygen contribution from the SFC membrane in the Pt/$CeZrO_2$ test: the SFC membrane serves more as an oxygen exchange medium like the $CeZrO_2$ support rather than as a net supplier of oxygen like the BSCF membrane.

The effect of the high flux BSCF membrane, on the other hand, differs more from the effect of the SFC membrane with the Pt/$CeZrO_2$ catalyst than with the Pt/ZrO_2 catalyst. The BSCF membrane not only produces higher and more enduring methane conversion levels than the SFC membrane, it also yields much more water production, much less CO_2 conversion, and somewhat higher

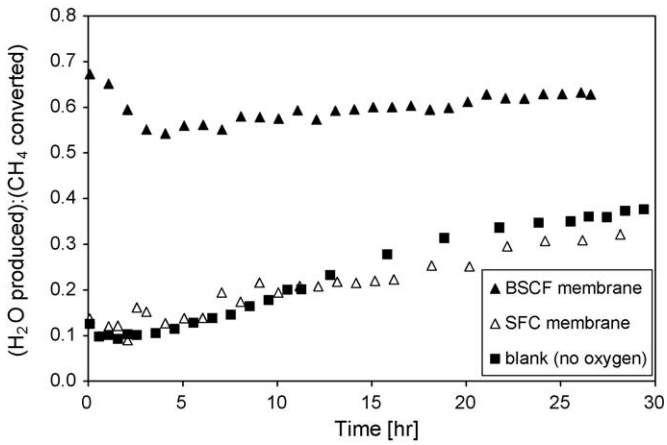

Fig. 12. Relative water production with the Pt/$CeZrO_2$ catalyst during CO_2 reforming at 800 °C. Feed flow is: 10 mL/min CH_4, 10 mL/min CO_2, and 5 mL/min argon; space velocity of 150 L/h/$g_{catalyst}$.

H_2:CO ratios. For example, after 25 h of reaction, methane conversion on the BSCF membrane with the Pt/$CeZrO_2$ catalyst is about 50% higher than on the SFC membrane and the H_2:CO ratio is about 25% higher, while CO_2 conversion is less than half and water production is about twice their respective values with the SFC membrane.

3.5. Reaction profile evaluation

The higher oxygen flux of the BSCF membrane anticipates the theoretical possibility of more partial oxidation of methane and its H_2:CO ratio of two, which means more partial oxidation should increase both methane conversion and H_2:CO ratio. Such an effect is observed with the BSCF membrane and the Pt/$CeZrO_2$ catalyst. However, partial oxidation does not produce water, so some combination of combustion, hydrogen oxidation on the membrane, and RWGS is required to explain the additional water production.

The low CO_2 conversion and high H_2:CO ratio eliminate the possibility of significant RWGS activity with the BSCF membrane and the Pt/$CeZrO_2$ catalyst. Combustion is a possible co-reaction with CO_2 reforming for this test, although it does not appear likely for any of the other tests. A combination of hydrogen oxidation and steam reforming seems most likely because of the previously discussed observations of membrane activity with no catalyst and the improbable oxygen transport requirements of combustion.

The proposition that both methane partial oxidation and hydrogen oxidation occur simultaneously on either membrane seems unlikely given the low activity of the membrane in the presence of methane and its high activity with hydrogen. We propose that hydrogen oxidation is the most likely oxygen consumption reaction at the membrane surface in all circumstances.

This proposal leads directly to the suggestion that some amount of steam reforming is occurring in the catalyst bed with the BSCF membrane whenever there is the appearance of partial oxidation. An equal combination of hydrogen oxidation and steam reforming yields identical product stoichiometry to partial oxidation. Hydrogen oxidation on the membrane could therefore account for all of the membrane oxygen consumption as long as some of the water produced participates in steam reforming to achieve the net effect and appearance of partial oxidation.

Steam reforming, partial oxidation, and combustion all diminish relative CO_2 conversion, with combustion having the most dramatic effect because it produces CO_2 while converting methane. With both catalysts, relative CO_2 conversion is much lower with the BSCF membrane than with the SFC membrane, indicating a significant difference in the mode(s) of methane conversion. The possibility of combustion increases with the amount of available oxygen, and the high flux BSCF membrane thus offers a greater potential for combustion than the low flux SFC membrane.

Relative water production is high on the BSCF membrane with the Pt/$CeZrO_2$ catalyst (Fig. 12) but not so with the Pt/ZrO_2 catalyst (Fig. 8). This too indicates the possibility of combustion as a contributing reaction. Relative hydrogen production rates offer the final evidence to include combustion in the reaction profile for the Pt/$CeZrO_2$ catalyst with the BSCF membrane. As shown in Fig. 13, relative hydrogen production is initially lower for this test than for the other tests and remains low throughout the test. This, in conjunction with the low relative CO_2 conversion, confirms that combustion is a likely contributor to methane conversion for the Pt/$CeZrO_2$ catalyst on the BSCF membrane. Conversely, the same catalyst with the SFC membrane was the only combination of catalyst and membrane that exhibited relatively high hydrogen production throughout.

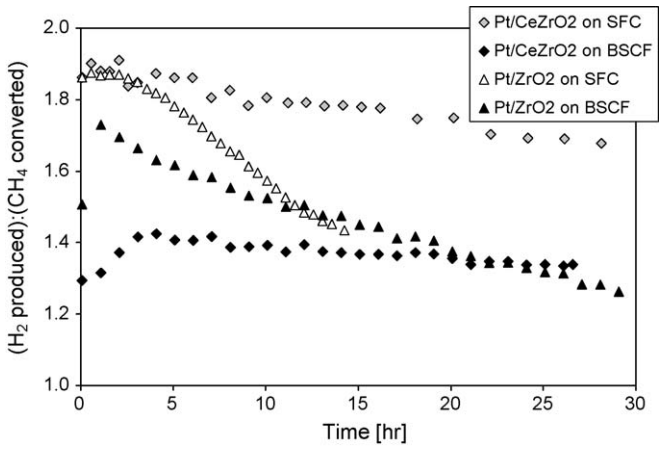

Fig. 13. Relative hydrogen production during CO_2 reforming at 800 °C. Feed flow is: 10 mL/min CH_4, 10 mL/min CO_2, and 5 mL/min argon; space velocity of 150 L/h/$g_{catalyst}$.

As the Pt/ZrO_2 catalyst tests progress, both approach the same level of relative hydrogen production as the $Pt/CeZrO_2$ on BSCF test (Fig. 13). However, in these two tests the decrease in relative hydrogen production is accompanied by an increase in relative CO_2 conversion. It appears that the Pt/ZrO_2 catalyst is generally more susceptible to RWGS activity than the $Pt/CeZrO_2$ catalyst while the $Pt/CeZrO_2$ catalyst is more likely to produce combustion with a high flux membrane than with a low flux membrane.

3.6. Membrane oxygen during reaction

Compared to membrane oxygen production under the air:argon oxygen potential gradient, only one of the test scenarios results in an increase in net membrane oxygen production: the BSCF membrane's apparent oxygen flux increases by 250% during reaction with the $Pt/CeZrO_2$ catalyst (Fig. 14). The previously reported explanation for such an increase under reaction conditions is that the H_2 and CO produced during reaction create a reducing environment that decreases the oxygen potential of the reaction-side surface of the membrane below that of the inert argon environment. This reduced oxygen potential increases the oxygen potential gradient across the membrane which increases oxygen flux across the membrane [4].

However, we propose that a decrease in the oxygen content of the membrane surface and the presence of CO_2 as an oxygen source may also lead to the conversion of CO_2 to CO on the membrane surface if oxygen diffusion through the membrane cannot replenish the oxygen content of the reaction-side surface as quickly as it is depleted by hydrogen oxidation. This hypothesis explains the otherwise unexplained coincidence of zero (or negative) net oxygen flux from the SFC membrane coupled with increased catalyst activity on the SFC membrane.

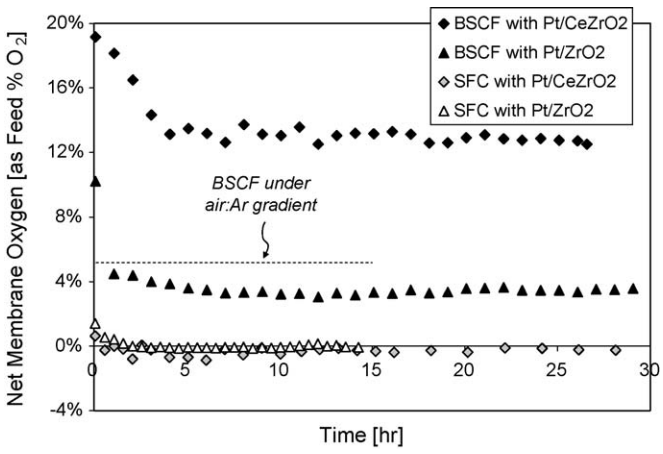

Fig. 14. Net membrane oxygen production during CO_2 reforming at 800 °C. Feed flow is: 10 mL/min CH_4, 10 mL/min CO_2, and 5 mL/min argon; space velocity of 150 L/h/$g_{catalyst}$.

Given the lack of membrane activity in the tests without catalyst, the proposed CO_2 reduction should only occur following reduction of the membrane surface by hydrogen oxidation, so the net effect of the proposed interfacial reactions is equivalent to Reverse Water-Gas Shift. However, this apparent RWGS via hydrogen oxidation and CO_2 reduction on the SFC surface is mechanistically different than conventional gas-phase RWGS in the catalyst bed.

The Pt/ZrO_2 results provide the justification for this conclusion: if RWGS occurred solely in the catalyst bed, the SFC membrane trends should be similar to the blank trends in Figs. 5–9. The trends clearly are not the same, yet the net membrane oxygen production is effectively zero with the Pt/ZrO_2 catalyst and is more often negative than positive with the $Pt/CeZrO_2$ catalyst (Fig. 14). The combination of no net oxygen contribution from the SFC membrane and the significantly different reaction profiles for the blank and SFC membrane tests supports the conclusion that the distinguishing reactions occur on the membrane surface.

The CO_2 reduction hypothesis can also explain why the BSCF membrane exhibits lower flux during steady state reaction with Pt/ZrO_2 than under the air:argon gradient (Fig. 14). Any imbalance between hydrogen oxidation and CO_2 reduction on the membrane yields either a positive or a negative contribution to net membrane oxygen production. The relative CO_2 conversion for Pt/ZrO_2 on BSCF is almost 50% higher than the relative CO_2 conversion for $Pt/CeZrO_2$ on BSCF while the relative water production is less throughout most of the test period. This discrepancy supports the possibility of the uptake of oxygen from CO_2 by the membrane and the accompanying negative contribution to net membrane oxygen production. Similarly, the low flux SFC membrane produces oxygen too slowly to surpass the oxygen removal rate from hydrogen oxidation and thus exhibits zero or negative values for net oxygen production.

4. Conclusions

Pre- and post-reaction membrane integrity testing with helium confirmed that dense SFC and bilayer BSCF membranes with good mechanical integrity and stability can be fabricated and used for reforming reactions on the laboratory scale. As expected, the BSCF membranes exhibited significantly higher flux than the SFC membranes and the $Pt/CeZrO_2$ catalyst was significantly more active than the Pt/ZrO_2 catalyst. Both low and high flux membranes improved catalyst longevity as well as activity with both catalysts.

The effect on methane conversion was generally proportional to the apparent oxygen production of the membrane. Neither membrane showed significant activity without the powder catalyst, nor did the blank membrane.

The membranes exhibited the potential with both powder catalysts to produce more water than the blank membrane tests. Higher water production is attributed to membrane oxidation of hydrogen and appears to induce steam reforming under certain conditions, based on net reactant consumption and product stoichiometry. The reaction test results provide indirect but consistent supporting evidence for the hypothesis that, under reforming reaction conditions, membrane oxygen reacts with hydrogen at the membrane surface rather than leaving the membrane as gaseous O_2.

Acknowledgement

Financial support for this project was provided by the Office of Naval Research (N00014-03-1-0601).

References

[1] W. Wang, S.M. Stagg-Williams, F.B. Noronha, L.V. Mattos, F.B. Passos, Catalysis Today 98 (2004) 553.
[2] K. Tomishige, Catalysis Today 89 (4) (2004) 405.
[3] S.J. Feng, S. Ran, D.C. Zhu, W. Liu, C.S. Chen, Energy & Fuels 18 (2004) 385.
[4] U. Balachandran, J.T. Dusek, P.S. Maiya, B. Ma, R.L. Mieville, M.S. Kleefisch, C.A. Udovich, Catalysis Today 36 (1997) 265.
[5] P.N. Dyer, R.E. Richards, S.L. Russek, D.M. Taylor, Solid State Ionics 134 (2000) 21.
[6] H.J. Bouwmeester, Catalysis Today 82 (2003) 141.
[7] D.A. Slade, A.M. Duncan, K.J. Nordheden, S.M. Stagg-Williams, Green Chemistry 9 (2007) 577.
[8] J.T. Ritchie, J.T. Richardson, D. Luss, AIChE Journal 47 (9) (2000) 2092.
[9] J.J. Spivey, Proceedings of the 232nd American Chemical Society National Meeting, San Francisco, California, September 2006, paper no. 136.
[10] C.-Y. Tsai, A.G. Dixon, W.R. Moser, Y.H. Ma, AIChE Journal 43 (11A) (1997) 2741.
[11] J.H. Bitter, K. Seshan, J.A. Lercher, Journal of Catalysis 171 (1997) 279.
[12] S.M. Stagg-Williams, F. Noronha, G. Fendley, D.E. Resasco, Journal of Catalysis 194 (2) (2000) 240.
[13] Z. Shao, W. Yang, Y. Cong, H. Dong, J. Tong, G. Xiong, Journal of Membrane Science 172 (2000) 177–188.
[14] M. Ikeguchi, K. Ishii, Y. Sekine, E. Kikuchi, M. Matsukata, Materials Letters 59 (11) (2005) 1356–1360.